

Full Paper

DNA double-strand break repair in *Penaeus monodon* is predominantly dependent on homologous recombination

Shikha Srivastava¹, Sumedha Dahal¹, Sharanya J. Naidu¹, Deepika Anand², Vidya Gopalakrishnan¹, Rajendran Kooloth Valappil^{2,*}, and Sathees C. Raghavan^{1,*}

¹Department of Biochemistry, Indian Institute of Science, Bangalore 560 012, India and ²ICAR-Central Institute of Fisheries Education, Mumbai 400 061, India

*To whom correspondence should be addressed. +91 22 2631 0657. Fax: +91 22 2631 0573. E-mail: rajendrankv@hotmail.com (R.K.V.); Tel. +91 80 22932674. Fax. +91 80 23600814. Email: sathees@biochem.iisc.ernet.in (S.C.R.)

Edited by Dr. Osamu Ohara

Received 8 August 2016; Editorial decision 3 December 2016; Accepted 8 December 2016

Abstract

DNA double-strand breaks (DSBs) are mostly repaired by nonhomologous end joining (NHEJ) and homologous recombination (HR) in higher eukaryotes. In contrast, HR-mediated DSB repair is the major double-strand break repair pathway in lower order organisms such as bacteria and yeast. *Penaeus monodon*, commonly known as black tiger shrimp, is one of the economically important crustaceans facing large-scale mortality due to exposure to infectious diseases. The animals can also get exposed to chemical mutagens under the culture conditions as well as in wild. Although DSB repair mechanisms have been described in mammals and some invertebrates, its mechanism is unknown in the shrimp species. In the present study, we show that HR-mediated DSB repair is the predominant mode of repair in *P. monodon*. Robust repair was observed at a temperature of 30 °C, when 2 µg of cell-free extract derived from hepatopancreas was used for the study. Although HR occurred through both reciprocal recombination and gene conversion, the latter was predominant when the bacterial colonies containing recombinants were evaluated. Unlike mammals, NHEJ-mediated DSB repair was undetectable in *P. monodon*. However, we could detect evidence for an alternative mode of NHEJ that uses microhomology, termed as microhomology-mediated end joining (MMEJ). Interestingly, unlike HR, MMEJ was predominant at lower temperatures. Therefore, the results suggest that, while HR is major DSB repair pathway in shrimp, MMEJ also plays a role in ensuring the continuity and stability of the genome.

Key words: Nonhomologous DNA end joining, MMEJ, Microhomology, Double-strand break, homologous recombination

1. Introduction

DNA in every living organism is constantly exposed to a plethora of mutagens including radiation, chemicals or oxidative stress leading to induction of a variety of DNA damages. Among different DNA damages, single- and double-strand breaks are considered as most hazardous, if not repaired or misrepaired.^{1–5} Depending upon the multitude of genotoxic lesions, a variety of DNA repair pathways have been evolved, namely excision repair [nucleotide excision repair (NER), base excision repair (BER) and mismatch repair (MMR)], which deals with DNA damage at the level of base and nucleotides, and DNA strand break repair, which helps in the repair of both single- and double-strand breaks.^{1–3,5–7}

DNA double-strand breaks (DSBs) occur when both strands of DNA duplex are broken in close vicinity. Improper repair of DSBs could result in genome rearrangements, loss of genetic information etc., while no repair may lead to cell death.^{8–12} In higher eukaryotes, nonhomologous end joining (NHEJ) is one of the major double-strand break repair pathways.^{5,10,12,13} Homologous recombination (HR) pathway is helpful in error-free DSB repair and is active at late S and G2 phases of cell cycle.^{5,10,12–14} Unlike HR, NHEJ helps in the maintenance of genome stability throughout all phases of cell cycle.^{15–17} A backup pathway to NHEJ, often referred as microhomology-mediated end joining (MMEJ) also exists in mammals. Till recently, it was believed that alternative NHEJ operates only in the absence of classical NHEJ;^{7,12,18–22} however, recent studies suggest that MMEJ can operate in parallel to classical NHEJ, albeit with low efficiency.²²

Penaeid species comprise the largest group of farmed crustaceans, with global production of approximately 3.4 million ton and Asia accounts for 90% of global shrimp aquaculture. Shrimp is the most important seafood product traded internationally; however, shrimp cultivation has been severely affected by a number of pathogens, mainly viruses, throughout the world. Based on the estimates, it was predicted that up to 40% of tropical shrimp production worth >\$3 billion is lost annually due to viral pathogens alone,²³ and ~80% production losses are due to disease occurrence in Asia.²⁴ Besides, shrimp can also get exposed to various chemicals with potential mutagenic effect, which are either used intentionally for health management purposes or through contaminated water sources. Being invertebrates, it is believed that shrimp do not possess acquired immunity, and are dependent on innate immune response. Although attempts are on to identify defense related host genes, information on DNA repair pathways and DNA repair genes is largely unknown.

MjRad23, a Rad23 homolog of NER pathway protein was identified and characterized in *Marsupenaeus japonicus*, a crustacean.²⁵ UVB radiation-induced damage and repair was also investigated in another crustacean, *Tigriopus japonicus*. An increased expression of proteins associated with classical NHEJ, HR, BER and MMR was observed.²⁶ In *Daphnia*, the DNA damage caused by UVB radiation is repaired by photoenzymatic mechanism, while NER was observed only at lower temperature.²⁷ Complete genome sequence of *Drosophila* revealed presence of various critical DNA repair proteins depending on their sequence similarity to other species.²⁸ While important NHEJ proteins, Ku70 and Ku80 orthologs were present in *Drosophila*,²⁹ DNA-dependent protein kinase (DNA-PK) catalytic subunit was absent suggesting an aberrant NHEJ/nonclassical NHEJ pathway in *Drosophila*.²⁸

Penaeus monodon, the black tiger shrimp, is one of the most economically important crustaceans. In the present study, we investigated various DSB repair mechanisms in *P. monodon*. We report

that HR-mediated DSB repair is the major DSB repair process in shrimp, while classical NHEJ is absent. Although HR occurred through both reciprocal recombination and gene conversion, the latter was predominant. To our surprise, we could detect evidence for an alternative mode of NHEJ named as MMEJ, which uses microhomology for joining. Hence, present study reveals that HR is the major DSB repair pathway in shrimps.

2. Materials and methods

2.1. Enzymes, chemicals and reagents

Chemical reagents were obtained from Sigma Chemical Co. (St. Louis, MO, USA), Amresco (USA), SRL (India) and Himedia (India). Radioisotope-labelled nucleotides were purchased from BRIT (Hyderabad, India).

2.2. Shrimp samples

Healthy shrimp, *P. monodon* (25–33 g), were obtained from Shakthi Aqua Farm Pvt. Ltd. Mumbai, Maharashtra (Fig. 1A). Shrimp were kept in 500-l FRP tanks containing sea water (14 ± 2 ppt salinity) with continuous aeration and maintained at 25–30°C. The collected animals were fed on commercially available pellet diet and acclimatized for 4–5 days before the experiment.³⁰ Hepatopancreas was collected from a group of three to four animals and pooled together for the experiments (Fig. 1B). The animals were screened for white spot syndrome virus (WSSV), the most pathogenic and prevalent pathogen infecting shrimp, using standard PCR method before starting the experiments.

2.3. Oligomers

The oligomers used in the study were purified using 8–15% denaturing PAGE as described before.³¹ 5'-end labelling of the oligomer was performed as described previously.³² T4 polynucleotide kinase was used and incubated in appropriate buffer containing [γ -³²P] ATP at 37°C for 1 h. The labelled substrates were purified using G-25 Sephadex columns and stored at –20°C until use.

2.4. Preparation of DNA substrates for NHEJ and MMEJ

For NHEJ study, oligomeric DNA substrate (SCR19), of length 75 nt was radiolabelled with [γ -³²P] ATP and annealed with unlabelled complementary strand, SCR20 in the presence of 100 mM NaCl and 1 mM EDTA as described earlier to prepare DSBs bearing 5' compatible overhangs.^{33,34} The substrates containing 5'–5' and 5'–3' noncompatible overhangs were prepared by annealing radiolabelled SCR19 with cold oligomer, VK11 and VK13, respectively.³⁵ Blunt ended substrate was prepared by annealing radiolabelled VK7 and cold oligomer, VK8.³⁵

For MMEJ studies, DNA substrates containing 10 nt microhomology regions were synthesized and prepared as described earlier.^{21,22} The complementary oligomers were annealed to generate double stranded DNA containing microhomology region. SS54 was annealed to SS62, and SS65 was annealed to SS66 to generate 10 nt microhomology region. MMEJ junctions were PCR amplified using radiolabelled SS60 and unlabelled SS61 primer.

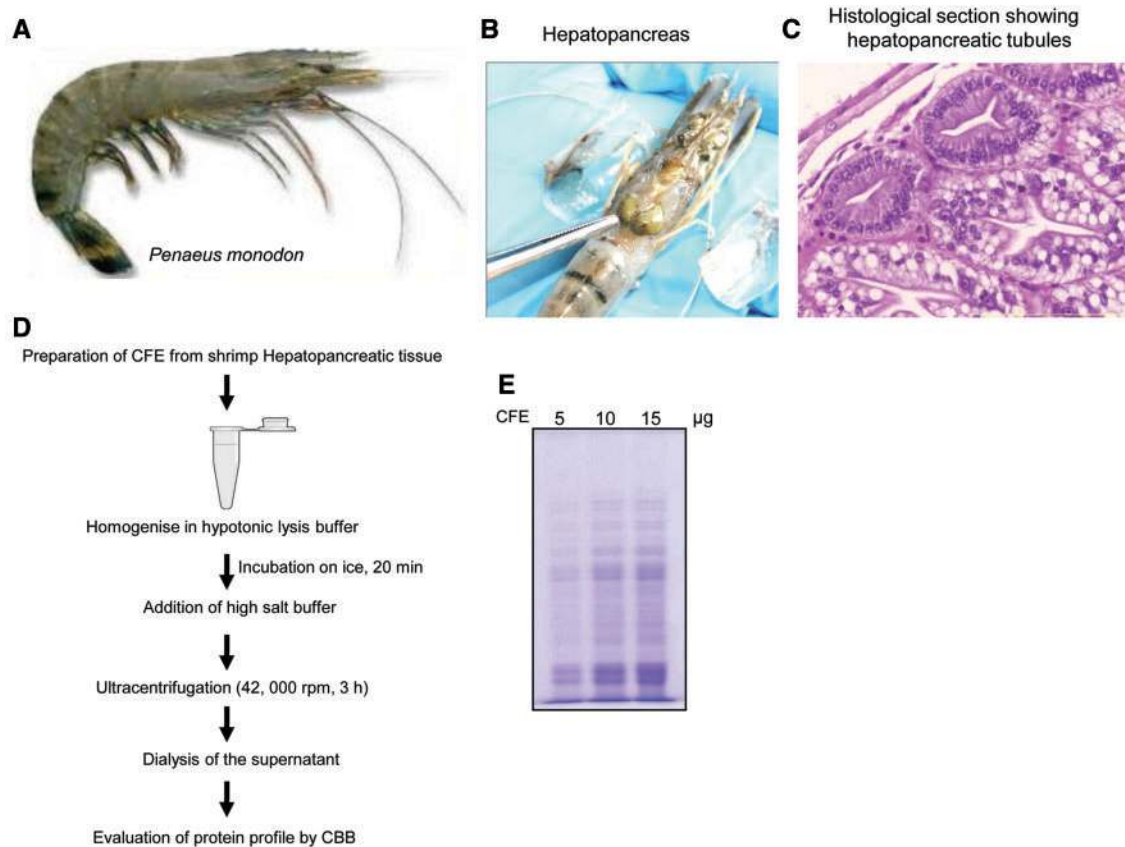


Figure 1. Preparation of cell-free extract (CFE) of hepatopancreas of shrimp, *P. monodon* and evaluation of protein profile. (A) Image showing black tiger shrimp, *Penaeus monodon*. (B) Dorsal view of dissected out shrimp showing hepatopancreas. (C) Histological section of hepatopancreas showing the tubular architecture and different types of cells of hepatopancreatic tubules. (D) Schematic representation of steps involved in the preparation of cell-free extract from hepatopancreas of *P. monodon*. (E) CBB staining showing protein profile of cell-free extracts of hepatopancreas. Different concentrations of CFE (5, 10, 15 µg) were resolved on a denaturing SDS-PAGE and stained with CBB stain.

2.5. Preparation of shrimp hepatopancreatic cell-free extract (CFE)

Cell-free extract was prepared from shrimp hepatopancreas in ice-cold conditions as described previously with modification.^{21,22,36} Briefly, tissues were minced with sterile scalpel and washed in ice-cold phosphate buffer saline. The cells were then resuspended in hypotonic lysis buffer [10 mM Tris-HCl (pH 8.0), 1 mM EDTA, 5 mM DTT] and were homogenized in 100 µl of hypotonic lysis buffer in the presence of protease inhibitors (phenylmethylsulfonyl fluoride, 0.01 M; aprotinin, 2 µg/ml; pepstatin, 1 µg/ml; leupeptin, 1 µg/ml) and incubated on ice for 20 min. The extract was centrifuged at 42,000 rpm for 3 h at 4°C in Beckman TLA-100 rotor after addition of 50 µl of high salt buffer [50 mM Tris-HCl (pH 7.5), 1 M KCl, 2 mM EDTA, 2 mM DTT]. The supernatant was dialysed overnight against dialysis buffer [20 mM Tris-HCl (pH 8.0), 0.1 M KOAc, 20% glycerol, 0.5 mM EDTA and 1 mM DTT]. Protein concentration was determined by Bradford assay, aliquoted and stored at -80°C till use.

2.6. NHEJ assay

NHEJ assay was performed using plasmid as described previously.³⁷⁻³⁹ Supercoiled pUC18 plasmid was digested with *EcoRI* to generate DSBs with cohesive ends. The plasmid DNA (600 ng) was incubated with increasing concentration of cell-free extract (0.5, 1,

1.5, 2, 4 and 8 µg) and incubated at 30°C for 6 h in 1× NHEJ buffer containing 30 mM HEPES-KOH (pH 7.9), 7.5 mM MgCl₂, 2 mM ATP, 1 mM DTT, 50 µM dNTPs, 100 mg/ml BSA, 10% PEG and 5% glycerol. Reaction was terminated (10 mM EDTA), products were purified by phenol-chloroform extraction and resolved on 1% agarose gel. NHEJ assay performed using rat testicular extract served as a positive control. The gel was visualized following staining with ethidium bromide and image was captured using gel documentation system (UVITEC, Cambridge, UK).

The NHEJ assay using oligomeric DNA was performed as described previously with modifications.^{33,35,39} Cell-free extract prepared from shrimp hepatopancreas was incubated with radiolabelled DNA substrates along with (or without) cold oligomeric DNA substrates (2 µM) at 30°C for 1 h (or as specified) in 1× NHEJ buffer. The reaction was terminated and the products were purified as described above. The purified products were resolved on 8% denaturing PAGE. The gels were dried, exposed onto the screen, and scanned using phosphorImager (FLA9000, Fuji, Japan). Analyses of data were done using Multigauge software (version 3).

Radioactive PCR was carried out after end-joining reaction to improve the sensitivity of the assay. Following end joining of different oligomeric DNA substrates bearing DSBs either compatible or non-compatible ends, catalysed by cell-free extract of shrimp hepatopancreas (0.5 µg; 30°C for 1 h), NHEJ junctions were amplified using radiolabelled oligomer, VK24 (5'-CCGGTACTACTCGAGCC-3')

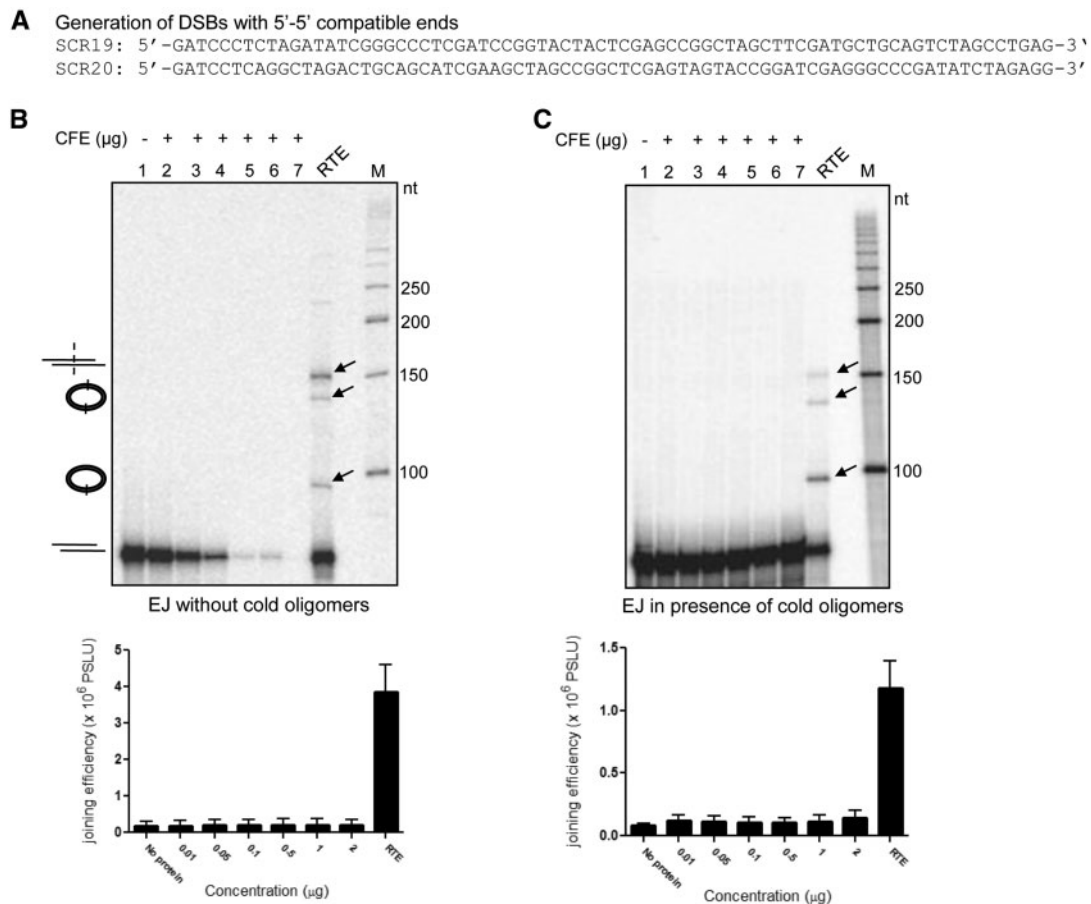


Figure 2. Evaluation of compatible DNA end joining catalysed by extracts of hepatopancreas of shrimp. (A) Sequence of oligomeric DNA bearing 5'-5' compatible ends used for the EJ study. (B, C) Evaluation of DNA end joining efficiency using increasing concentrations of CFE (0.01, 0.05, 0.1, 0.5, 1 and 2 μg) of hepatopancreas using 5'-5' compatible end substrate (B) and in presence of additional cold oligomers (C). DNA incubated with rat testicular extract (RTE) was used as a positive control. Lane 1 is no protein control and 'M' is 50 nt DNA ladder. Bar diagram showing quantitation of EJ efficiency along with the error bar (SEM). Intensity of the band was calculated and expressed in PSL units. Arrow indicates joined products; circular form I (monomer), linear dimer and circular form II (dimer) are shown.

and unlabelled SS37 (5'-TGCAGCATCAAGCTAGCC-3'). The reaction products were resolved on 8% denaturing PAGE and radioactive signals were detected as described above.

2.7. MMEJ assay

MMEJ assay was performed as described earlier.^{21,22,34} The reaction was carried out in a volume of 20 μl containing MMEJ buffer [50 mM Tris-HCl (pH 7.6), 20 mM MgCl_2 , 1 mM DTT and 1 mM ATP]. The DNA substrates bearing 10 nt microhomology were incubated along with hepatopancreatic CFE at 30°C for 2 h (or as specified). Reaction was terminated by heat denaturing at 65°C (for 20 min) and the end-joined products were detected by radioactive PCR using radiolabelled oligomer, SS60 and unlabelled SS61. The reaction products were resolved on 8% denaturing PAGE and radioactive signals were detected using phosphorImager, as described above.

2.8. HR assay

In vitro HR assay was performed as described previously, using two independent plasmids.^{38,40,41} Two plasmid constructs, pTO223 and pTO231, were generated by introducing mutations to neomycin

resistant gene on pTO221 as described.⁴⁰ Briefly, pTO223 was created by deleting a 245-bp (*NarI*) segment from 5' region of *neomycin* (*neo* Δ 2) gene and pTO231 was created by deleting 282 bp (*NaeI*) segment from 3' of *neomycin* (*neo* Δ 1). In pTO223, *neo* gene was flanked by *EcoRI* and *SalI* restriction enzyme sites. *HindIII* site was also present close to *EcoRI* at 5' end, which was absent in pTO231. pTO221 was generated using pBSKS where 1.5 kb of *HindIII/SalI* restriction fragment of pBR322::Tn5 containing the *neo* gene was inserted at the same restriction sites. pTO223 and pTO231 carried functional ampicillin resistant gene and served as substrates for the assay.

The HR assay was performed using 500 ng of each plasmids (pTO223 and pTO231) by incubating with increasing concentrations of shrimp hepatopancreatic extracts (0, 0.5, 1, 1.5, 2 and 4 μg) in a buffer containing 35 mM HEPES (pH 8.0), 10 mM MgCl_2 , 1 mM DTT, 2 mM ATP, 50 μM dNTPs, 1 mM NAD and 100 $\mu\text{g/ml}$ BSA at 30°C (or as specified) for 30 min. Reaction was terminated by adding EDTA (20 mM) and reaction products were purified using phenol-chloroform extraction. Purified DNA was used for the transformation of *E. coli* DH5 α and plated over agar plates containing ampicillin and kanamycin antibiotics, and scored for transformants and recombinants, respectively. For all the experiments, no protein

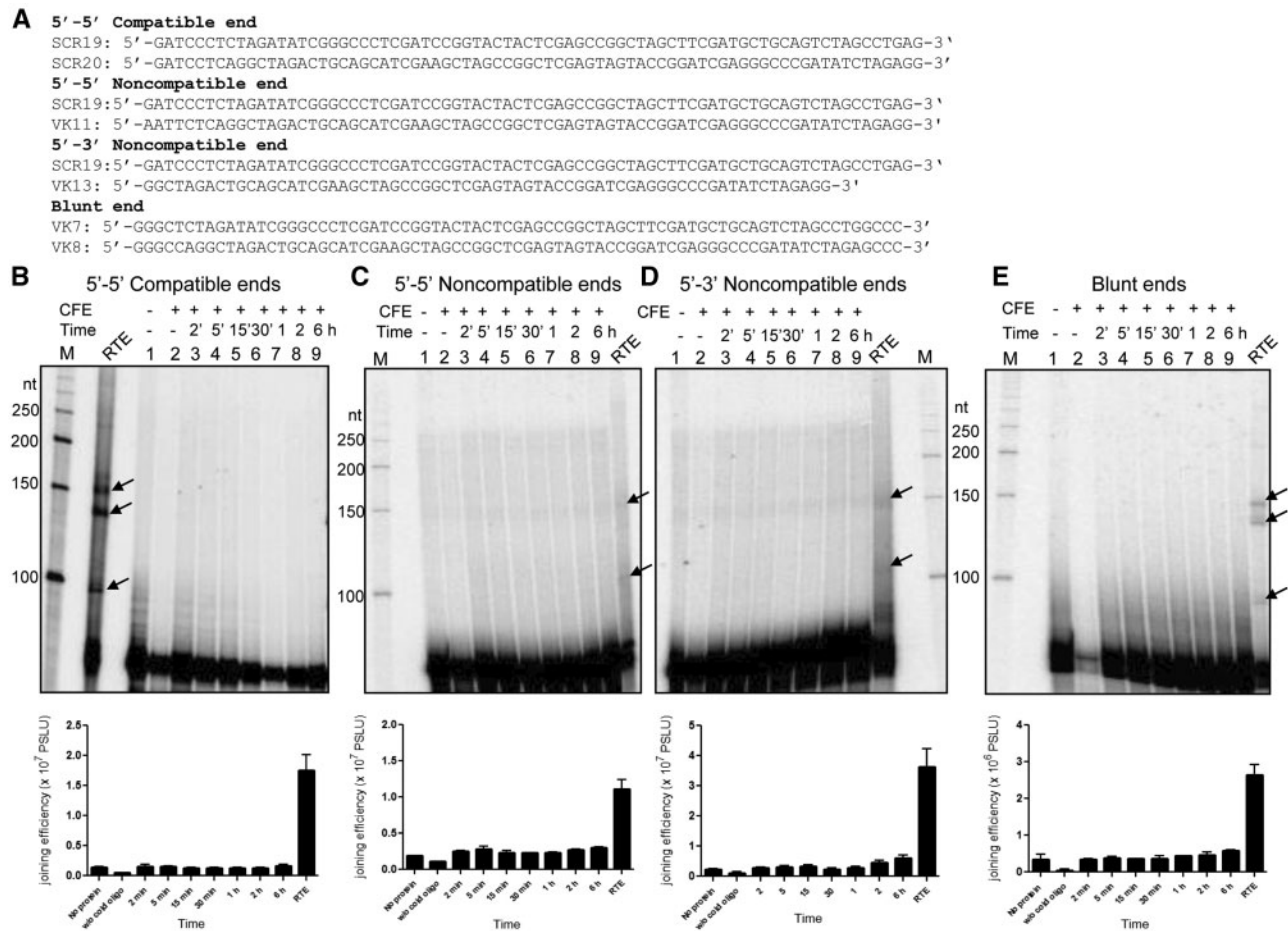


Figure 3. Efficacy of end joining catalysed by extracts of hepatopancreas of shrimp, compared with oligomeric DNA bearing DSBs with different end structures. (A) Sequence of different oligomeric DNA substrates used for the NHEJ reaction. (B-E) Time kinetics of NHEJ catalysed by shrimp hepatopancreatic extracts (0.5 μ g), when treated with 5'-5' compatible end, (B) 5'-5' noncompatible end (C), 5'-3' noncompatible end (D) and blunt end (E) DNA substrates incubated for 2, 5, 15, 30 min and 1, 2 and 6 h. Products were resolved on denaturing PAGE. RTE treated samples served as positive control for respective type of DNA breaks. Lane 1 is no protein control and 'M' is 50 nt DNA ladder. In each panel, bar diagram displaying quantitation of NHEJ products is shown with error bar (SEM; $n = 3$). Joining products are indicated by arrow as circular form I (monomer), linear dimer and circular form II (dimer).

control served as negative control, which accounts for background recombination catalysed by *E. coli*. The recombination frequency was calculated as ratio of number of recombinants to the number of transformants per microgram of DNA.

2.9. Restriction enzyme digestion analysis to distinguish reciprocal exchange and gene conversion

Kanamycin resistant colonies containing recombinants were confirmed for functional *neo* gene by restriction endonuclease digestion. Functional *neo* gene can be formed by reciprocal exchange or gene conversion. In reciprocal exchange, a crossing over within the region between deletions *neo* Δ 1 and *neo* Δ 2 takes place giving rise to functional *neo*⁺ allele and a non-functional double mutant allele. In gene conversion a transfer of DNA from *neo* Δ 1 to *neo* Δ 2 takes place giving rise to functional *neo* gene. Restriction digestion of pTO223 and pTO231 will give rise to a 1.25- and 1.2-kb fragments, respectively, when digested with *Eco*RI-*Sal*I and is indicative of *neo* Δ 2 and *neo* Δ 1 allele and a 2.9-kb fragment corresponding to vector DNA. In contrast, digestion of plasmids containing *neo* gene will release a 1.5-kb fragment that is indicative of the presence of functional *neo* gene.

3. Results

3.1. Cell-free system to study DNA repair pathways

Cell-free extract was prepared from hepatopancreas of healthy tiger shrimp, *P. monodon* for studying DSB repair pathways (Fig. 1A and B). The hepatopancreas was chosen as the target tissue in the experiment, as this is the primary organ responsible for absorption and storage of ingested material and involved in the synthesis of digestive enzymes and detoxification of xenobiotics. The organ constitutes 2-6% of the body weight and consists of hepatopancreatic tubules (Fig. 1C). Cell-free extract was prepared based on previously published work,^{21,22,36} protein profile was examined on a CBB gel, and used for DSB repair studies (Fig. 1D and E).

3.2. Unlike mammals, classical NHEJ is absent in *P. monodon*

To test for the presence of classical NHEJ in the extracts of hepatopancreas of *P. monodon*, an oligomeric DNA based assay system was employed in addition to plasmid-joining assay (Fig. 2 and data not shown). In order to optimize the oligomer-based assay system, different parameters were tested using oligomeric DNA substrate

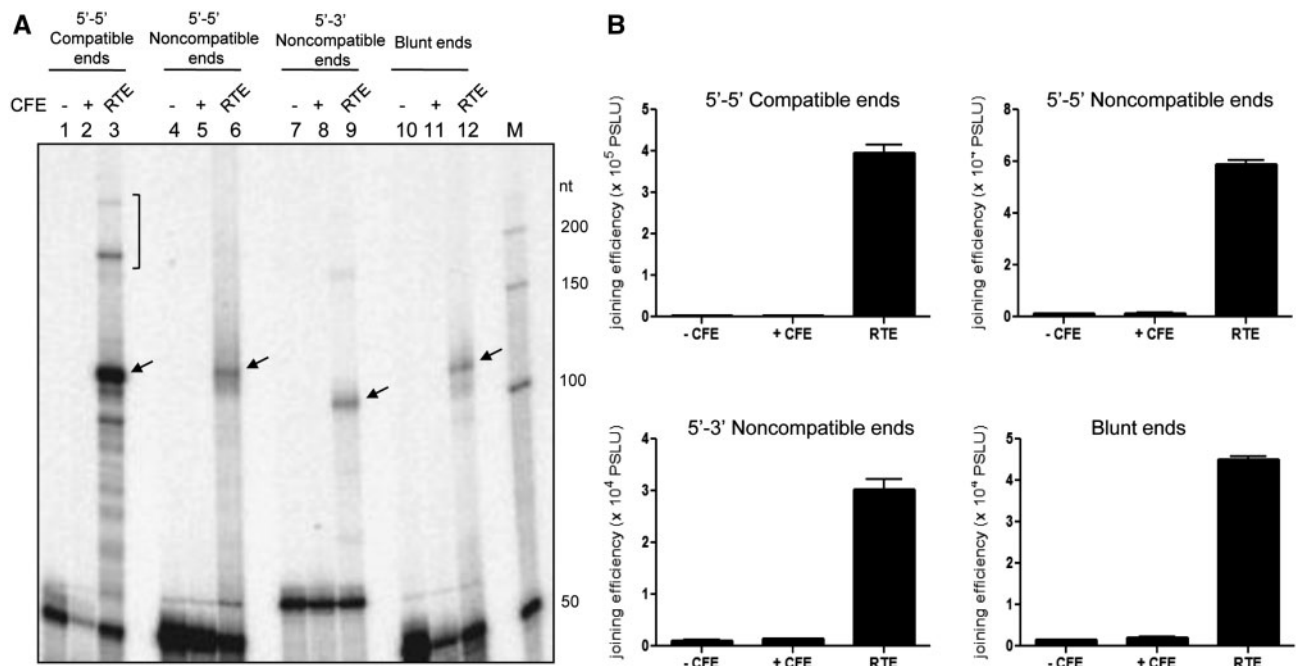


Figure 4. Evaluation of end joining catalysed by hepatopancreas extract of shrimp following radioactive PCR. (A) Different oligomeric DNA substrates (5'-5' compatible, 5'-5' noncompatible, 5'-3' noncompatible and blunt end) were incubated with shrimp hepatopancreas CFE. The presence of end-joined products was examined through radioactive PCR. Amplified products were resolved on 8% denaturing PAGE. Lane 1, 4, 7, 10 are no protein control. Rat testicular extract treated samples served as positive controls. (B) Bar diagram displaying quantitation of joined products with error bar (SEM; $n=3$) indicated. Band intensity was calculated and expressed in PSLU units. Joined products are indicated by arrow. Multimers are shown in bracket. 'M' is 50 nt DNA ladder.

bearing 5'-5' compatible ends (Fig. 2A). [γ - 32 P] ATP-labelled oligonucleotides were incubated (30°C, 1 h) with increasing concentrations of hepatopancreas cell-free extract and purified products were resolved on denaturing PAGE (Fig. 2B). Results showed no joined products upon treatment with the hepatopancreas cell extracts, unlike the positive controls in which the testicular extract prepared from rat showed end to end joining of 75 mer DNA leading to both circular and linear multimeric products (Fig. 2B).^{21,33,35,39} Although hepatopancreatic extracts did not exhibit DNA end joining, it possessed efficient nuclease activity leading to degradation of substrate DNA, in a protein concentration-dependent manner (Fig. 2B). Furthermore, unlabelled random double-stranded DNA was added to the end-joining reaction mix to reduce the nuclease activity. Although this helped in reducing the nuclease activity on labelled DNA significantly, hepatopancreas cell extract did not exhibit joining of DSBs possessing compatible ends even after incubating with increasing concentrations of the extract (Fig. 2C).

To further evaluate the end-joining efficiency of hepatopancreas extract, oligomeric DNA having different types of DSBs, such as substrates possessing 5'-5' compatible end, 5'-5' non-compatible end, 5'-3' non-compatible end and blunt ends, were incubated with extracts (0.5 μ g) (Fig. 3A) in the presence of cold double-stranded DNA at different time points (2, 5, 15, 30 min, 1, 2 and 6 h). Analysis of purified products on denaturing PAGE confirmed no end-to-end joining of any of the DNA substrates tested (Fig. 3B-E), although end joining was observed in the case of rat testicular extracts, as reported previously.³⁵

Since we failed to detect any end-joined products using *in vitro* NHEJ analysis, radioactive PCR was employed to improve the sensitivity of the assay. Oligomeric DNA substrates bearing DSBs (5'-5' compatible, 5'-5' non-compatible, 5'-3' non-compatible or blunt

ends) were incubated with shrimp hepatopancreas cell-free extract (0.5 μ g) and resolved on denaturing PAGE following radioactive PCR (Fig. 4A and B). Results showed efficient joining in case of rat testicular extracts (positive control), while no amplification of joined products was observed in the case of shrimp hepatopancreas extract (Fig. 4). Thus, we conclude that cell-free extract from *P. monodon* was unable to catalyse DSB joining through NHEJ, irrespective of the type of DSBs used for analysis suggesting the absence of functional classical NHEJ in shrimps.

3.3. *Penaeus monodon* possesses detectable microhomology mediated DNA end joining (MMEJ)

Since classical NHEJ was not detected in *P. monodon*, we investigated whether DSB repair can occur using microhomology as reported recently in rodents.^{22,34} To test this hypothesis, we synthesized DNA with 10 nt microhomology region and experiment was carried out as outlined (Fig. 5A and B).²² DNA substrates bearing microhomology were incubated with increasing concentrations of shrimp hepatopancreas extracts or with heat inactivated extracts for 2 h. Products were resolved on a denaturing PAGE, following radioactive PCR using labelled primer (Fig. 5C). Results showed a distinct product at 62 bp position (indicated by arrow) suggesting the joining through MMEJ (Fig. 5C). Although the efficiency of the joining catalysed by extracts of hepatopancreas was lesser compared with the positive control, testicular extract from rat; it was dependent on concentration of hepatopancreatic extracts (Fig. 5D). A distinct band due to MMEJ was observed, when as low as 0.1 μ g of hepatopancreas extract was used. An increase in efficiency was observed with increasing concentration of CFE, and 0.5 μ g of extract was noted as optimal (Fig. 5D). A decrease in joining efficiency was

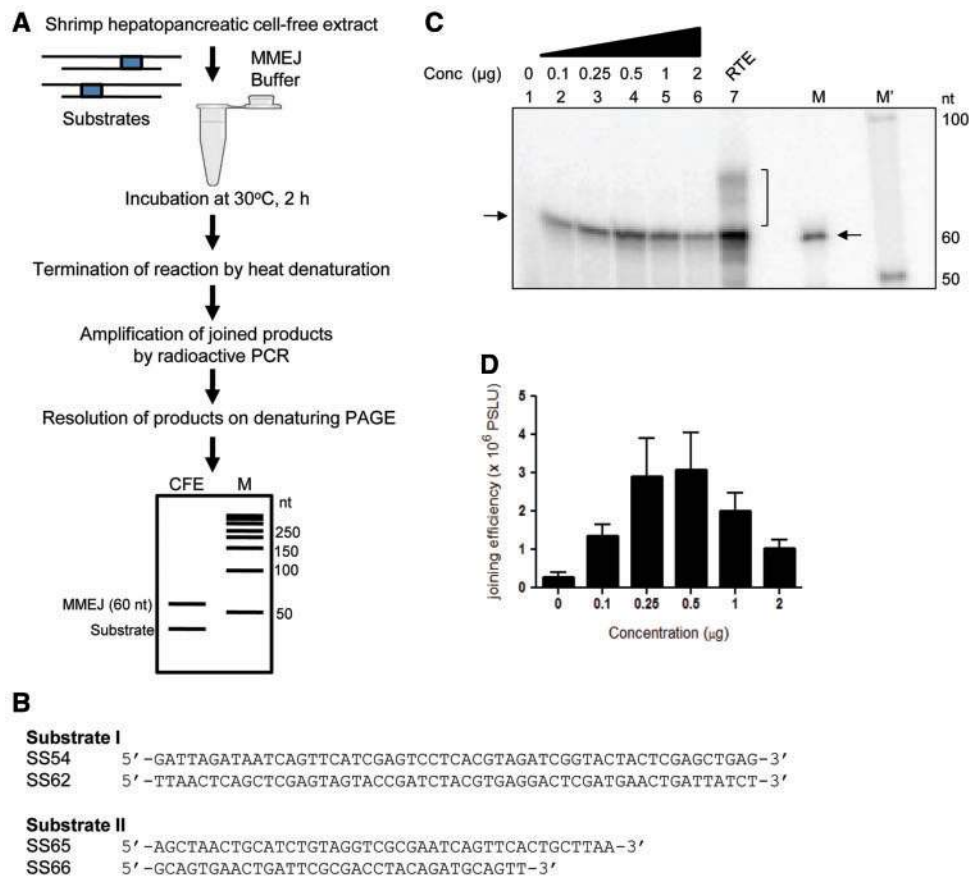


Figure 5. Efficiency of MMEJ catalysed by increasing concentrations of shrimp hepatopancreatic extract. (A) Schematic showing experimental strategy used for evaluating MMEJ in shrimp hepatopancreatic extract. Double-stranded oligomeric DNA possessing 10 nt microhomology region was used as DNA substrates as indicated and incubated with buffer and extracts at 30°C for 2 h. Following termination of reaction, MMEJ products were amplified using radioactive PCR following labelling of one of the primers. PCR products were resolved on 8% denaturing PAGE and a characteristic 62 nt product indicates joining due to MMEJ. (B) DNA sequence of oligomers used for the study and 10 nt microhomology regions are indicated. (C) PAGE profile showing MMEJ products following incubation of DNA substrates with increasing concentrations of shrimp hepatopancreatic extracts (0.1, 0.25, 0.5, 1 and 2 µg). Lane 1 is no protein control and RTE treated sample was used as positive control. MMEJ product was indicated by arrow. (D) Bar diagram showing error bar (SEM; $n=3$) based on the quantitation of multiple biological repeats of MMEJ reaction. The intensity of bands was calculated and expressed in PSL units. C-NHEJ products are shown in bracket. 'M' is 60 nt marker and 'M' is 50 nt DNA ladder.

observed at high concentrations of CFE (1 and 2 µg), which could be due to increased levels of nuclease activity.

3.4. MMEJ occurs efficiently at lower temperature and starts within 2 min of addition of hepatopancreas extract

In order to determine optimal incubation time for efficient MMEJ catalysed by hepatopancreatic extracts, 0.5 µg of extract was incubated with DNA substrates possessing 10 nt microhomology for various time periods (2, 5, 15, 30 min, 1, 2, 6 h). Results showed that robust joining due to MMEJ was observed as early as 2 min, however, incubation up to 2 h and beyond resulted in reduced joining (Fig. 6A and B). To check the optimal temperature for MMEJ catalysed by the shrimp hepatopancreatic extracts, the DNA substrate and protein extracts were incubated at various temperatures (4, 16, 25, 30 and 37°C). Results showed robust MMEJ at lower temperature. An increase in temperature to 30°C or above resulted in reduced efficiency of joining, most likely due to loss of DNA because of nuclease activity (Fig. 6C and D). Therefore, various lines of

experiments suggest that hepatopancreas extract of *P. monodon* possesses MMEJ, although classical NHEJ was undetectable.

3.5. HR-mediated DSB repair is efficient in *P. monodon*

Since DSB repair mediated through MMEJ results in deletion of sequence between microhomology regions, this could result in deletions in genome and hence genomic instability. Therefore, we were interested in investigating the mechanism by which genomic stability is maintained. To test this, HR-mediated DSB repair was evaluated in hepatopancreas extract of *P. monodon* using plasmid-based assay system. Two plasmids with two independent mutations at neomycin gene (pTO223 and pTO231) were used to evaluate DSB repair catalysed through HR (Fig. 7A). The plasmids were incubated with hepatopancreatic extracts in HR buffer and purified DNA was transformed in *E. coli* DH5 α . Recombinants were scored on kanamycin containing agar plates. Recombination catalysed by the extracts, will result in the restoration of functional *neo*⁺ gene conferring resistance to kanamycin upon transformation in recombination deficient, *E. coli* (*recA*⁻ strain of DH5 α F⁻).

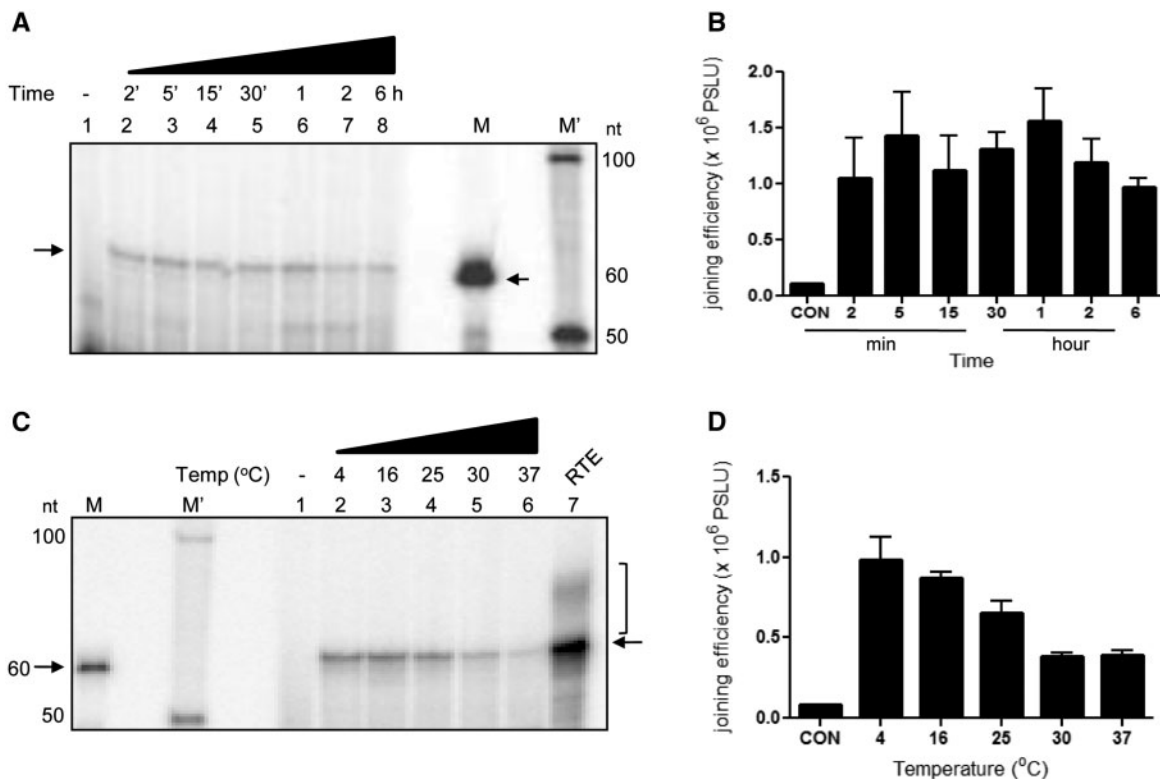


Figure 6. Evaluation of MMEJ catalysed by hepatopancreatic extracts of shrimp at different incubation time and temperature. (A) PAGE profile showing time kinetics of MMEJ, when 10 nt microhomology DNA substrate was used. Shrimp hepatopancreatic extracts (0.5 μ g) were incubated at 30°C for different time points (2, 5, 15, 30 min, 1, 2, 6 h). (B) Bar diagram with error bar (SEM) showing quantitation of MMEJ products at different time points ($n=3$). (C) PAGE profile showing efficiency of MMEJ catalysed by extracts of shrimp hepatopancreas (0.5 μ g) at different temperature (4, 16, 25, 30 and 37°C) incubated for 2 h. (D) Bar diagram showing error bar (SEM) of MMEJ products at different temperature ($n=3$). C-NHEJ products are shown in bracket. 'M' is 60 nt marker and 'M' is 50 nt DNA ladder.

HR assay was performed by incubating shrimp hepatopancreatic extracts (2 μ g) along with pTO223 and pTO231. DNA treated with heat inactivated extracts served as the control (Fig. 7B). No protein control acted as negative control for bacterial recombination efficiency. Results showed efficient recombination catalysed by hepatopancreas extract, which was \sim 200-fold higher than the recombination frequency of no protein control and heat inactivated extract control (Fig. 7B). Importantly, the observed HR efficiency was $>$ 30-fold higher than that of HR efficiency of mouse testicular extract (Fig. 7B). Therefore, cell-free extract of hepatopancreas is proficient in HR-mediated DSB repair.

Further protein titration was performed to determine the optimal extract concentration for HR-mediated DSB repair activity. Results showed a concentration (0.5, 1, 1.5, 2, 4 μ g) dependent increase in the recombination frequency (Fig. 7D). We have also checked the effect of temperature on the efficiency of HR-mediated DSB repair. Hepatopancreas extract (0.5 μ g) was incubated with pTO223 and pTO231 at different temperatures (4, 16, 24, 30, 37°C) for 30 min (Fig. 7C). The purified plasmids were transformed in *E. coli* and scored for recombinants as described above. Results showed the highest recombination frequency at 30 and 37°C. Efficiency of recombination was lowest at 4 and 42°C (data not shown), while it was moderate at 16 and 24°C. These results in conjunction with earlier results suggest that HR is predominant at the physiological temperature, while MMEJ efficiency is poor. In contrast, HR frequency was poor at lower temperature, whereas MMEJ efficiency was high.

3.6. HR-mediated recombination in hepatopancreas extracts occurs through gene conversion and reciprocal exchange

Recombinant clones were evaluated for joining through reciprocal recombination and gene conversion by restriction enzyme digestion. During reciprocal exchange, a crossing over within the region between deleted neomycin gene, *neo* Δ 1 and *neo* Δ 2 takes place, giving rise to functional *neo*⁺ allele and a nonfunctional double mutant allele. In contrast during gene conversion, a transfer of DNA from *neo* Δ 1 to *neo* Δ 2 takes place, giving rise to functional *neo* gene. When digested with *Eco*RI–*Sal*I, pTO223 and pTO231 can give rise to a 1.25- and 1.2-kb fragments, respectively, and is indicative of *neo* Δ 2 and *neo* Δ 1 allele (Fig. 8A). In contrast, digestion of plasmids containing *neo* gene will result in release of a 1.5-kb fragment that is indicative of presence of functional *neo* gene.

Upon *Hind*III–*Sal*I double digestion, release of 1.25 kb fragment from pTO223 was observed, which was similar to that of *Eco*RI–*Sal*I digestion, while a larger 4.1-kb fragment was released from pTO231 due to the absence of *Hind*III site (Fig. 8A) (when digested, pTO231 gets linearized with *Sal*I giving rise to single large 4.1 kb fragment). Upon HR, the *neo* gene comprising *neo* Δ 1 allele lacking *Hind*III site and right part of *neo* Δ 2 allele with *Sal*I site resulted in the absence of 1.5 kb fragment, which was seen upon *Eco*RI–*Sal*I double digestion. In contrast, during gene conversion, transfer of DNA fragment from *neo* Δ 1 to *neo* Δ 2 allele takes place, and therefore, *Hind*III–*Sal*I digestion resulted in the release of a 1.5-kb

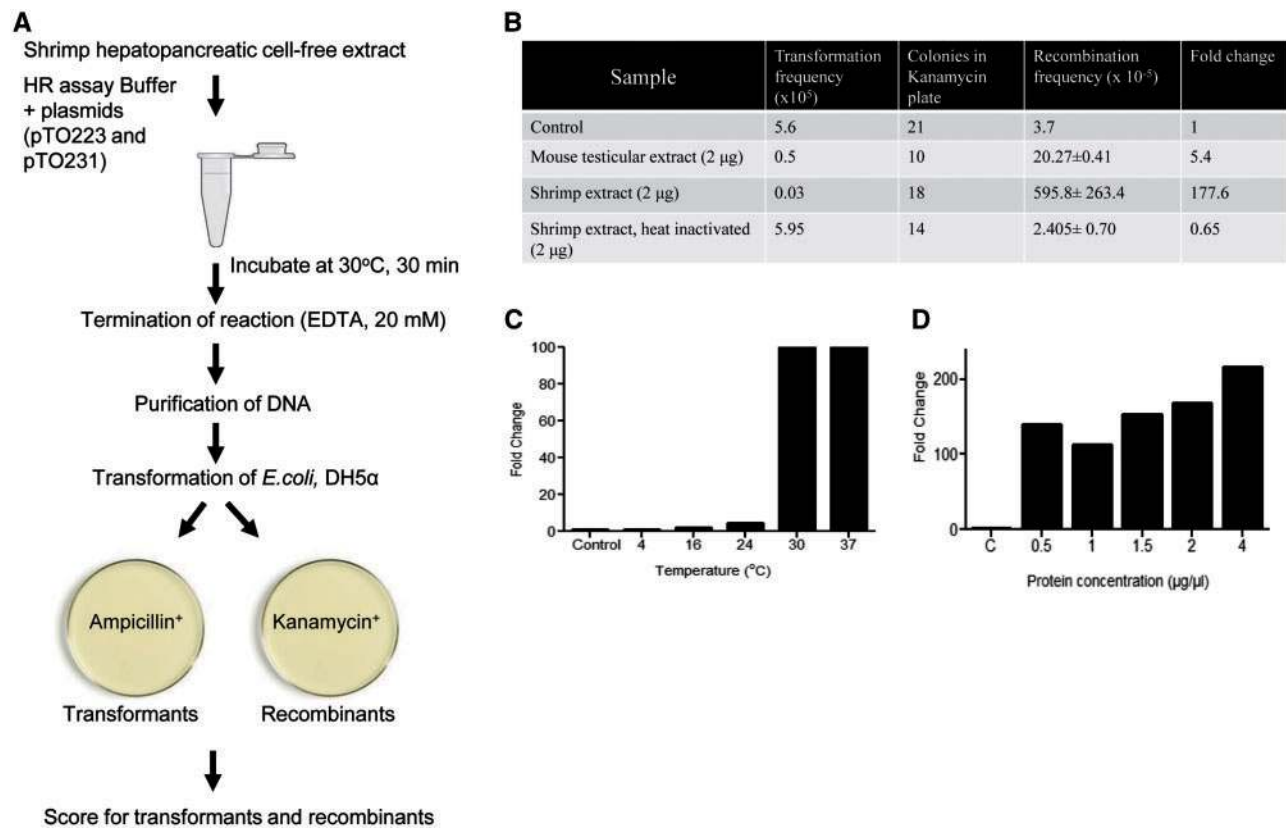


Figure 7. Evaluation of HR-mediated DSB repair catalysed by hepatopancreas extracts. (A) Schematic presentation showing plasmid based HR assay. Plasmids (pTO223 and pTO231) were incubated with shrimp hepatopancreas CFE in HR assay buffer at 30°C for 30 min. Purified DNA was used for transformation of *E. coli* DH5 α and plated on agar plates containing ampicillin to determine transformation efficiency and kanamycin to calculate recombination frequency. (B) Table showing *in vitro* recombination catalysed by hepatopancreas extract and its heat inactivated form. Mouse testicular extracts acted as a positive control. (C) Efficacy of HR-mediated DSB repair in shrimp hepatopancreatic extract when examined at different incubation temperatures. Hepatopancreatic extracts (0.5 μ g) were incubated with substrate DNA at different temperature (4, 16, 24, 30, 37°C). (D) Bar diagram showing recombination frequencies catalysed by increasing concentrations (0.5, 1, 1.5, 2, 4 μ g) of shrimp hepatopancreas extract. 'C' is no protein control.

fragment. Thus, the release of a 1.5-kb fragment during *EcoRI*–*SalI* digestion is indicative of the presence of functional *neo* gene (Fig. 8B), while a release of 1.5 kb fragment due to *HindIII*–*SalI* digestion is indicative of wild-type *neo* gene due to gene conversion (Fig. 8C). However, it is important to note that gene conversion between *neo* Δ 2 to *neo* Δ 1, cannot be scored upon *HindIII*–*SalI* digestion and therefore, observed frequency of gene conversion could be an under representation.

These observations revealed that HR-mediated DSB repair occurred using both gene conversion and reciprocal exchange. Among the clones analysed, in >60% of the cases HR was through gene conversion (Fig. 8D). Therefore, our results suggested that DSB repair in *P. monodon* is dependent on HR and microhomology-mediated DNA end joining (Fig. 9). However, unlike mammals classical NHEJ was undetectable (Fig. 9).

4. Discussion

Multiple DNA repair pathways have evolved to combat DNA damage, ensuring survival of a cell.^{2,3,10} From prokaryotes to lower eukaryotes and to higher eukaryotes, several of these DNA repair pathways are conserved. Several DNA repair proteins also show high degree of amino acid homology across the living world. However, there are several organisms, where DNA repair pathways

are unexplored due to various reasons including non-conservation of polypeptides or lack of complete genome sequence making the study of DNA repair a challenge.

In the present study, we investigated DSB repair pathways in one of the crustaceans, *P. monodon*, using a cell-free assay system of one of the most important organs, hepatopancreas. Using the cell free-extract, which contains almost all the cellular proteins, we observed that NHEJ, the major DSB repair pathway in mammals is undetectable in the crustaceans. Interestingly, the more precise and faithful, HR-mediated repair is predominant and efficient. Although classical NHEJ was absent, a recently described backup NHEJ, known as MMEJ is functional in this organism. However, the protein machinery involved in each of these DNA repair pathway needs to be investigated.

4.1. HR is proficient in *P. monodon*

Unlike other DSB repair mechanisms, HR-mediated repair results in faithful joining of broken DNA without nucleotide loss. Although NHEJ is the predominant DSB repair mechanism in mammals, HR is the major DSB repair pathway in prokaryotes, and lower eukaryotes. Interestingly, we observed that HR-mediated DSB repair is highly efficient in *P. monodon*. Interestingly, we observed >30-fold higher recombination frequency, when extracts of shrimp hepatopancreas was compared with testicular extract. This is indeed remarkable and

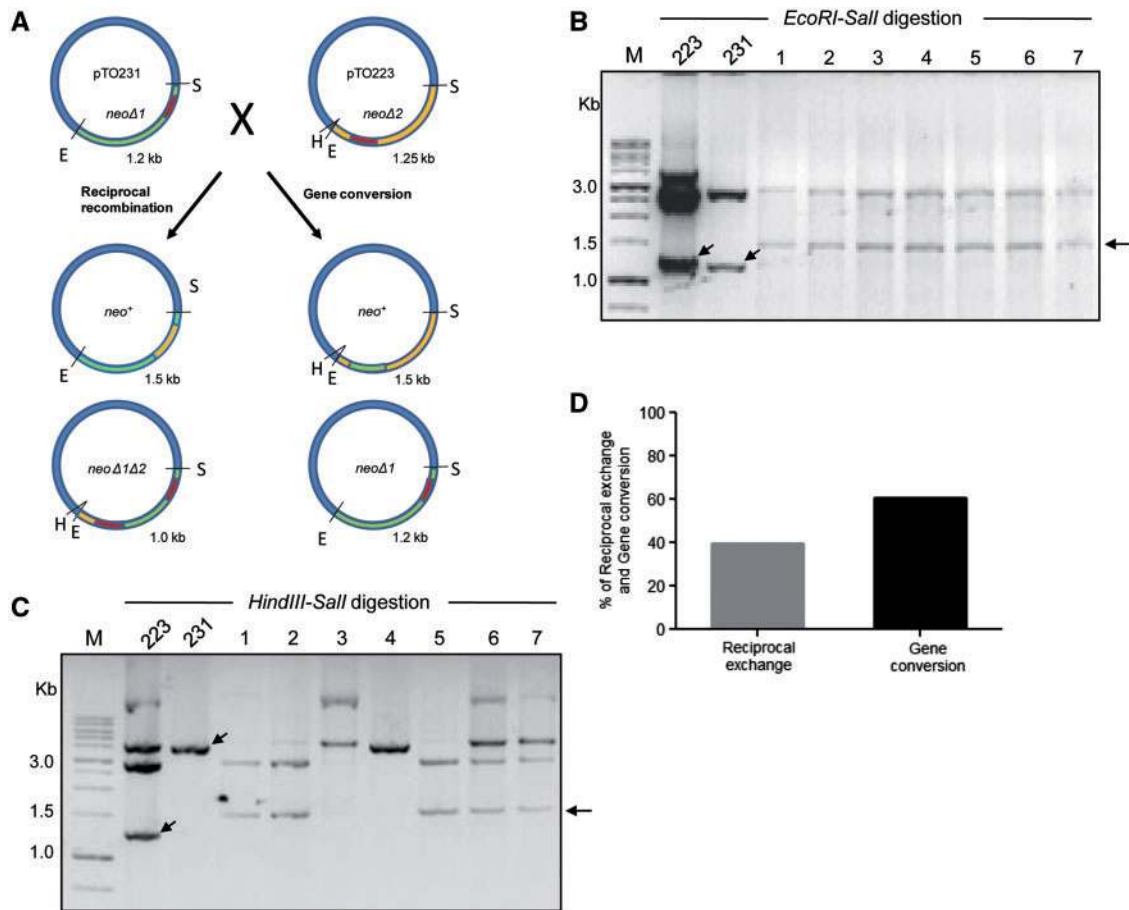


Figure 8. Evaluation of molecular mechanism of HR-mediated DSB repair in hepatopancreatic extract of shrimp. (A) Schematics showing reciprocal recombination and gene conversion-mediated HR that can lead to recreation of functional *neo* gene. *neoΔ1* in pTO231 and *neoΔ2* in pTO223 are nonfunctional *neomycin* genes. *neoΔ1* lacks *Nael* towards right side of the gene (shown in red) and *neoΔ2* lacks *Narl* towards the left side of the gene (shown in red). A crossing over between two mutants will give rise to a functional *neo* gene and a nonfunctional allele containing both the deletions. In the case of gene conversion, transfer of DNA from *neoΔ1* to *neoΔ2* takes place resulting in functional *neo* gene. *HindIII* site present adjacent to *EcoRI* site was destroyed in *neoΔ1*, hence *HindIII/SalI* resulting in 1.5 kb fragment occurs only at the time of gene conversion. (B) Representative agarose gel profile showing *EcoRI/SalI* restriction digestion of recombinant clones. Lanes 1–7 show release of fragment size of 1.5 kb of functional *neo* gene; 223 and 231 are mutant plasmids. (C) Agarose gel profile showing *HindIII/SalI* restriction digestion of recombinants. Lanes 1–7 show gene conversion releasing 1.5 kb of functional *neo* gene, except in the case of lane 4. Lane 3 showed a partially digested clone. 'M' is 1 kb DNA ladder. (D) Bar diagram showing frequency of HR-mediated DSB repair through either gene conversion or reciprocal recombination.

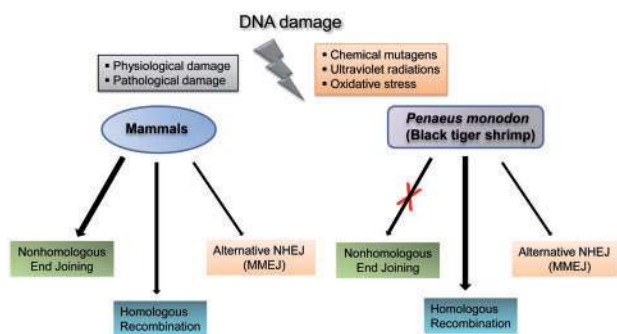


Figure 9. Cartoon depicting comparison of major DSB repair pathways in mammals and *Penaeus monodon*. Unlike mammals, HR and alternative NHEJ (MMEJ) are the major DNA break repair pathways in shrimp. Classical NHEJ and HR are the major DSB repair pathways in mammals, while MMEJ operates only at a low level.

underlines the importance of precise repair, and maintenance of integrity of the genome. Although a hepatopancreatic protein concentration-dependent increase in the recombination frequency was observed, recombination frequency was highest at 30 or 37°C and the efficiency was significantly less at lower temperature. There are several DNA repair proteins present in *Drosophila* that are reported to possess sequence similarity with other species. It was reported that HR is the predominant DSB repair pathway in mitotically dividing cells of *Drosophila*.⁴²

We noted that although HR-mediated DSB repair could occur through reciprocal exchange and gene conversion, in the case of *P. monodon*, the most preferred pathway was gene conversion (>60% of the cases). Considering that cell type used in the present study was of somatic cells, in hepatopancreas, this is understandable. In *E. coli*, RecA is the major component of DNA repair system. In *S. cerevisiae*, Rad51 family of proteins are present, which are similar to RecA proteins present in *E. coli*.²⁸ An ortholog of Rad51 has been found in

*Drosophila*⁴³ and another one closely related to human Xrcc3,⁴⁴ but *Drosophila* lacks Dmc1 ortholog. Although, we have not investigated the protein machinery involved in HR-mediated repair in shrimp, it is very much possible that RAD51 homologs will be playing a critical role. Similarly, homologs of MRE11, RAD50 and NBS1 also need to be investigated. Furthermore, it will be interesting to see whether RAD51 paralogues play any significant role in crustaceans.

4.2. MMEJ is preferred over classical NHEJ

The present study suggested that cell-free extracts prepared from hepatopancreas of *P. monodon* possess microhomology-mediated end joining, while classical NHEJ was undetectable. This is surprising, when one considers the fact that joining through MMEJ could lead to deletions in the genome culminating into genomic instability.^{12,18} It may be possible that NHEJ proteins such as Ligase IV/XRCC4, Ku70/Ku80, Artemis, DNA-PKcs etc., may be absent or expressed low in crustaceans, although it needs to be verified. Similarly, it will be interesting to look at the levels of MMEJ proteins such as Ligase III, PARP1, FEN1 in *P. monodon*.

Previously, it has been suggested that MMEJ operates in those cells, which are devoid of C-NHEJ.^{12,18} Although, recent studies suggest that both classical NHEJ and MMEJ can coexist, this will be dependent on levels of protein expression. A synthesis-dependent microhomology-mediated end joining has been previously observed in *Drosophila*,^{45,46} which is consistent with our present study.

In our study, we observed that unlike HR-mediated repair, which was very efficient at 30°C and above, MMEJ was optimal at 4 and 16°C. Although the relevance of this observation is unclear, it appears that this could be one way of promoting HR-mediated repair to ensure genomic stability. More studies are needed to decipher the importance of MMEJ in crustaceans, as it may facilitate evolution, since it could lead to changes in the DNA sequences.

4.3. Does efficient repair protect crustaceans from infections?

There is a direct connection between DSB repair and immunoglobulin diversity during adaptive immune response in mammals. NHEJ is critical during the rearrangement of V(D)J subexons.^{47,48} Hence, NHEJ proteins such as KU complex and Ligase IV play a critical role in the generation of antibody diversity. Therefore, it will be interesting to evaluate, whether efficient repair system in crustaceans can protect these organisms from infections. Previous studies indicate that, DNA repair proteins may suppress viral infections, in higher organisms.⁴⁹ Studies suggest that DNA repair proteins may inhibit and can have an effect on retrotransposons and viral infections in yeast and mammals.^{50–52} Furthermore, both Rad52 and Rad18 have been reported to suppress HIV-1 infection.⁵² However, these aspects need to be further investigated in shrimp.

Choice of repair pathway takes place at several steps of DSB repair process. After initiation of processive end resection, NHEJ cannot take place,⁵³ while a choice between HR and SSA (single-strand annealing), which is Rad51 dependent, takes place in *Drosophila*. P-element-induced DSBs were shown to be efficiently repaired by MMEJ mechanism in wild-type *Drosophila* and were unaffected in lig4 mutant flies.⁵⁴

It will be very interesting and significant to understand whether these DNA repair machineries can protect crustaceans against infections. It is possible that certain mutations in the repair pathways make them susceptible to a particular infection. In other words, it

will be important to look at the DNA repair genes of crustaceans following viral infection to determine the cause of heavy mortality due to some of the viruses.

Authors' contributions

S.S., S.D., S.J.N., D.A., V.G., R.K.V. and S.C.R. conceived, designed and conducted the experiments, analysed the data and wrote the manuscript.

Acknowledgements

We thank M. Nambiar, S. Vartak, R. Sebastian and SCR laboratory members for critical reading of the manuscript.

Conflict of interest

None declared.

Funding

Financial assistance from IISc-DBT partnership programme [DBT/BF/PR/INS/2011-12/IISc] for SCR is acknowledged. S.S. is supported by Dr D. S. Kothari Postdoctoral Fellowship from UGC, India and S.D. is supported by IISc fellowship, Bangalore (India).

References

1. Srivastava, M. and Raghavan, S.C. 2015, DNA double-strand break repair inhibitors as cancer therapeutics. *Chem. Biol.*, **22**, 17–29.
2. Friedberg, E.C., Aguilera, A., Gellert, M., et al. 2006, DNA repair: from molecular mechanism to human disease. *DNA Repair*, **5**, 986–96.
3. Friedberg, E.C., Backendorf, C., Burke, J., et al. 1987, Molecular aspects of DNA repair. *Mutation Res*, **184**, 67–86.
4. Nambiar, M. and Raghavan, S.C. 2013, Chromosomal translocations among the healthy human population: implications in oncogenesis. *Cell. Mol. Life Sci*, **70**, 1381–92.
5. Sharma, S. and Raghavan, S.C. 2010, Nonhomologous DNA end joining in cell-free extracts. *J. Nucleic Acids*.
6. Lieber, M.R., Yu, K. and Raghavan, S.C. 2006, Roles of nonhomologous DNA end joining, V(D)J recombination, and class switch recombination in chromosomal translocations. *DNA Repair*, **5**, 1234–45.
7. Iliakis, G., Murmann, T. and Soni, A. 2015, Alternative end-joining repair pathways are the ultimate backup for abrogated classical non-homologous end-joining and homologous recombination repair: implications for the formation of chromosome translocations. *Mutat. Res. Genet. Toxicol. Environ. Mutagen.*, **793**, 166–75.
8. Nambiar, M. and Raghavan, S.C. 2011, How does DNA break during chromosomal translocations? *Nucleic Acids Res.*, **39**, 5813–25.
9. Javadekar, S.M. and Raghavan, S.C. 2015, Snaps and mends: DNA breaks and chromosomal translocations. *FEBS J.*, **282**, 2627–45.
10. Wyman, C. and Kanaar, R. 2006, DNA double-strand break repair: all's well that ends well. *Annu. Rev. Genet.*, **40**, 363–83.
11. Lieber, M.R., Raghavan, S.C. and Yu, K. 2008, Mechanistic aspects of lymphoid chromosomal translocations. *J. Natl. Cancer Inst. Monogr.*, **39**, 8–11.
12. Gostissa, M., Alt, F.W. and Chiarle, R. 2011, Mechanisms that promote and suppress chromosomal translocations in lymphocytes. *Ann. Rev. Immunol.*, **29**, 319–50.
13. Lieber, M.R. 2010, NHEJ and its backup pathways in chromosomal translocations. *Nat. Struct. Mol. Biol.*, **17**, 393–5.

14. Chapman, J.R., Taylor, M.R. and Boulton, S.J. 2012, Playing the end game: DNA double-strand break repair pathway choice. *Mol. Cell*, **47**, 497–510.
15. Lieber, M.R., Ma, Y., Pannicke, U. and Schwarz, K. 2003, Mechanism and regulation of human non-homologous DNA end-joining. *Nat. Rev. Mol. Cell. Biol.*, **4**, 712–20.
16. Ciccia, A. and Elledge, S.J. 2010, The DNA damage response: making it safe to play with knives. *Mol. Cell*, **40**, 179–204.
17. Orthwein, A., Fradet-Turcotte, A., Noordermeer, S.M., et al. 2014, Mitosis inhibits DNA double-strand break repair to guard against telomere fusions. *Science*, **344**, 189–93.
18. Simsek, D. and Jasin, M. 2010, Alternative end-joining is suppressed by the canonical NHEJ component Xrcc4-ligase IV during chromosomal translocation formation. *Nat. Struct. Mol. Biol.*, **17**, 410–6.
19. Iliakis, G. 2009, Backup pathways of NHEJ in cells of higher eukaryotes: cell cycle dependence. *Radiother. Oncol.*, **92**, 310–5.
20. Wu, W., Wang, M., Mussfeldt, T. and Iliakis, G. 2008, Enhanced use of backup pathways of NHEJ in G2 in Chinese hamster mutant cells with defects in the classical pathway of NHEJ. *Radiat. Res.*, **170**, 512–20.
21. Chiruvella, K.K., Sebastian, R., Sharma, S., Karande, A.A., Choudhary, B. and Raghavan, S.C. 2012, Time-dependent predominance of nonhomologous DNA end-joining pathways during embryonic development in mice. *J. Mol. Biol.*, **417**, 197–211.
22. Sharma, S., Javadekar, S.M., Pandey, M., Srivastava, M., Kumari, R. and Raghavan, S.C. 2015, Homology and enzymatic requirements of microhomology-dependent alternative end joining. *Cell Death Dis.*, **6**, e1697.
23. Stentiford, G.D., Neil, D.M., Peeler, E.J., et al. 2012, Disease will limit future food supply from the global crustacean fishery and aquaculture sectors. *J. Invertebr. Pathol.*, **110**, 141–57.
24. Flegel, T.W. 2012, Historic emergence, impact and current status of shrimp pathogens in Asia. *J. Invertebr. Pathol.*, **110**, 166–73.
25. Sudhakaran, R., Okugawa, S., Mekata, T., et al. 2011, Deciphering the DNA repair protein, Rad23 from kuruma shrimp *Marsupenaeus japonicus*: full-length cDNA cloning and characterization. *Letts. Appl. Microbiol.*, **53**, 63–72.
26. Rhee, J.S., Kim, B.M., Choi, B.S. and Lee, J.S. 2012, Expression pattern analysis of DNA repair-related and DNA damage response genes revealed by 55K oligomicroarray upon UV-B irradiation in the intertidal copepod, *Tigriopus japonicus*. *Comp. Biochem. Physiol. C. Toxicol. Pharmacol.*, **155**, 359–68.
27. Connelly, S.J., Moeller, R.E., Sanchez, G. and Mitchell, D.L. 2009, Temperature effects on survival and DNA repair in four freshwater cladoceran *Daphnia* species exposed to UV radiation. *Photochem. Photobiol.*, **85**, 144–52.
28. Sekelsky, J.J., Brodsky, M.H. and Burtis, K.C. 2000, DNA repair in *Drosophila*: insights from the *Drosophila* genome sequence. *J. Cell Biol.*, **150**, F31–6.
29. Beall, E.L. and Rio, D.C. 1996, *Drosophila* IRBP/Ku p70 corresponds to the mutagen-sensitive mus309 gene and is involved in P-element excision *in vivo*. *Genes Dev.*, **10**, 921–33.
30. Deepika, A., Sreedharan, K., Paria, A., Makesh, M. and Rajendran, K.V. 2014, Toll-pathway in tiger shrimp (*Penaeus monodon*) responds to white spot syndrome virus infection: evidence through molecular characterisation and expression profiles of MyD88, TRAF6 and TLR genes. *Fish Shellfish Immunol.*, **41**, 441–54.
31. Nambiar, M., Goldsmith, G., Moorthy, B.T. et al. 2011, Formation of a G-quadruplex at the BCL2 major breakpoint region of the t(14;18) translocation in follicular lymphoma. *Nucleic Acids Res.*, **39**, 936–48.
32. Nambiar, M. and Raghavan, S.C. 2012, Mechanism of fragility at BCL2 gene minor breakpoint cluster region during t(14;18) chromosomal translocation. *J. Biol. Chem.*, **287**, 8688–701.
33. Kumar, T.S., Kari, V., Choudhary, B., Nambiar, M., Akila, T.S. and Raghavan, S.C. 2010, Anti-apoptotic protein BCL2 down-regulates DNA end joining in cancer cells. *J. Biol. Chem.*, **285**, 32657–70.
34. Tadi, S.K., Sebastian, R., Dahal, S., Babu, R.K., Choudhary, B. and Raghavan, S.C. 2016, Microhomology-mediated end joining is the principal mediator of double-strand break repair during mitochondrial DNA lesions. *Mol. Biol. Cell*, **27**, 223–35.
35. Sharma, S., Choudhary, B. and Raghavan, S.C. 2011, Efficiency of non-homologous DNA end joining varies among somatic tissues, despite similarity in mechanism. *Cell. Mol. Life Sci.*, **68**, 661–76.
36. Baumann, P. and West, S.C. 1998, DNA end-joining catalyzed by human cell-free extracts. *Proc. Natl. Acad. Sci. U.S.A.*, **95**, 14066–70.
37. Sathees, C.R. and Raman, M.J. 1999, Mouse testicular extracts process DNA double-strand breaks efficiently by DNA end-to-end joining. *Mutat. Res.*, **433**, 1–13.
38. Raghavan, S.C. and Raman, M.J. 2004, Nonhomologous end joining of complementary and noncomplementary DNA termini in mouse testicular extracts. *DNA Repair*, **3**, 1297–310.
39. Srivastava, M., Nambiar, M., Sharma, S. et al. 2012, An inhibitor of non-homologous end-joining abrogates double-strand break repair and impedes cancer progression. *Cell*, **151**, 1474–87.
40. Oppliger, T., Wurgler, F.E. and Sengstag, C. 1993, A plasmid system to monitor gene conversion and reciprocal recombination *in vitro*. *Mutation Res.*, **291**, 181–92.
41. Srivastava, N. and Raman, M.J. 2007, Homologous recombination-mediated double-strand break repair in mouse testicular extracts and comparison with different germ cell stages. *Cell Biochem. Funct.*, **25**, 75–86.
42. Do, A.T., Brooks, J.T., Le Neveu, M.K. and LaRocque, J.R. 2014, Double-strand break repair assays determine pathway choice and structure of gene conversion events in *Drosophila melanogaster*. *G3 (Bethesda)*, **4**, 425–32.
43. McKee, B.D., Ren, X. and Hong, C.H. 1996, A recA-like gene in *Drosophila melanogaster* that is expressed at high levels in female but not male meiotic tissues. *Chromosoma*, **104**, 479–488.
44. Ghabrial, A., Ray, R.P. and Schupbach, T. 1998, okra and spindle-B encode components of the RAD52 DNA repair pathway and affect meiosis and patterning in *Drosophila oogenesis*. *Genes Dev.*, **12**, 2711–23.
45. Chan, S.H., Yu, A.M. and McVey, M. 2010, Dual roles for DNA polymerase theta in alternative end-joining repair of double-strand breaks in *Drosophila*. *PLoS Genet.*, **6**, e1001005.
46. Yu, A.M. and McVey, M. 2010, Synthesis-dependent microhomology-mediated end joining accounts for multiple types of repair junctions. *Nucleic Acids Res.*, **38**, 5706–17.
47. Nishana, M. and Raghavan, S.C. 2012, Role of recombination activating genes in the generation of antigen receptor diversity and beyond. *Immunology*, **137**, 271–81.
48. Nambiar, M., Kari, V. and Raghavan, S.C. 2008, Chromosomal translocations in cancer. *Biochim. Biophys. Acta*, **1786**, 139–52.
49. Zhao, F., Hou, N.B., Song, T. et al. 2008, Cellular DNA repair cofactors affecting hepatitis B virus infection and replication. *World J. Gastroenterol.*, **14**, 5059–65.
50. Scholes, D.T., Banerjee, M., Bowen, B. and Curcio, M.J. 2001, Multiple regulators of Ty1 transposition in *Saccharomyces cerevisiae* have conserved roles in genome maintenance. *Genetics*, **159**, 1449–65.
51. Irwin, B., Aye, M., Baldi, P., et al. 2005, Retroviruses and yeast retrotransposons use overlapping sets of host genes. *Genome Res.*, **15**, 641–54.
52. Yoder, K., Sarasin, A., Kraemer, K., McIlhatton, M., Bushman, F. and Fishel, R. 2006, The DNA repair genes XPB and XPD defend cells from retroviral infection. *Proc. Natl. Acad. Sci. U.S.A.*, **103**, 4622–7.
53. Symington, L.S. and Gautier, J. 2011, Double-strand break end resection and repair pathway choice. *Annu. Rev. Genet.*, **45**, 247–71.
54. McVey, M., Radut, D. and Sekelsky, J.J. 2004, End-joining repair of double-strand breaks in *Drosophila melanogaster* is largely DNA ligase IV independent. *Genetics*, **168**, 2067–76.